AIMS Energy, 13(3): 781–797.
DOI: 10.3934/energy.2025028
Received: 10 March 2025
Revised: 19 June 2025
Accepted: 24 June 2025
Published: 27 June2025

https://www.aimspress.com/journal/energy

Research article

Design of flywheel energy storage device with high specific energy

Hong Li[1], Xiaojiao Wang[1], Yueyi Li[1], Junjie Chen[1], Wanqi Wang[1] and Jiangwei Chu[2,*]

[1] College of Automotive Engineering, Beijing Polytechnic University, Beijing, 100176, China
[2] College of Mechanical and Electrical Engineering, Northeast Forestry University, Harbin 150040, China

*** Correspondence:** Email: cjw_62@nefu.edu.cn; Tel: +13624605621.

Abstract: The flywheel energy storage system is a way to meet the high-power energy storage and energy/power conversion needs. Moreover, the flywheel can effectively assist the hybrid drivetrain to meet the vehicle's large peak power requirements. For the automotive use of flywheels, it is particularly important to increase the moment of inertia of the flywheel as much as possible while keeping the overall mass increase low. In order to improve the specific energy of the system, a multi-stage flywheel rotor was designed. Consider a typical example here, such as $I = 3$, $\varepsilon = 0.96$, $\delta = 1.1$ (i, ε, δ represent the speed ratio, mass ratio and radius ratio of the two-stage flywheel), where four groups of secondary flywheels are installed in a flywheel energy storage device. Without considering the mass of the second stage gear, the specific energy of the flywheel device was 6.19 times that of the original flywheel device. If the mass of the second stage gear was considered, the value was 5.80. Moreover, for certain ε and δ, the specific energy of the proposed system was related to the size of i.

Keywords: energy storage; flywheel rotor; metallic material; specific energy

Nomenclature Units: I: inertia of the flywheel kg·m^2; ω_{max}, ω_{min}: flywheel maximum, minimum angular velocity rad/s; r, r_i, r_o: flywheel disc radius, inner radius, outer radius m; h: flywheel disc height m; ρ: *flywheel* density kg/m^3; μ: Poisson's ratio; m: disc total mass kg; $[\sigma]$: allowable tensile strength Mpa

1. Introduction

Typical energy storage technologies mainly include physical energy storage, electrochemical energy storage, and electromagnetic energy storage. At present, pumped energy storage (physical energy storage) accounts for 86.2% of the global total energy storage. The new model of energy storage

accounts for about 12.2%, in which the lithium-ion batteries are overwhelmingly dominant, with a market share of more than 90% [1]. Flywheel and compressed air energy storage account for less than 1% [1]. Pumped energy storage is mainly applied to the power grid side, which converts the excess electric energy when the power grid load is low into high-value electric energy during peak periods of the power grid, and is used for long-term and large-scale power supply. Flywheel energy storage has many advantages, such as high efficiency (up to 90%), large instantaneous power (single megawatt level), fast response speed (several milliseconds), long service life (100,000 cycles), and small environmental impact [2–4]. It is one of the most promising short-term high-power energy storage technologies.

To comprehend the development trend of "flywheel energy storage" technology, a literature search was conducted in the Engineering Village database, CNKI database and Web of Science database with the topic (All Fields) including "Flywheel Energy Storage" in this paper. The time span was 30 years (1990–2020). The annual publication volume, classification, and country (region) of the literatures are shown in Figure 1.

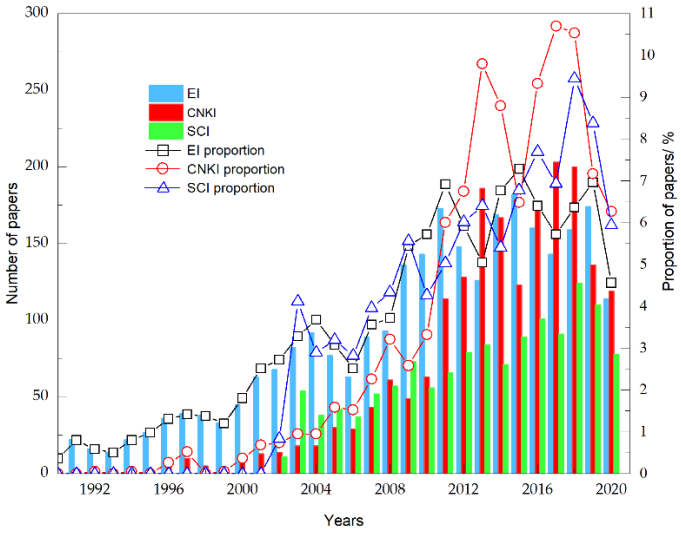

(a)

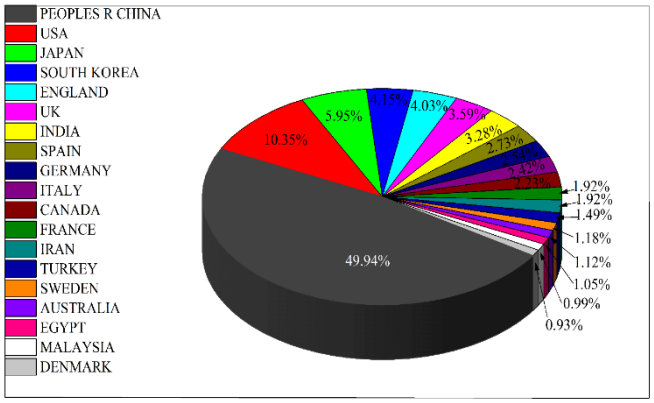

(b)

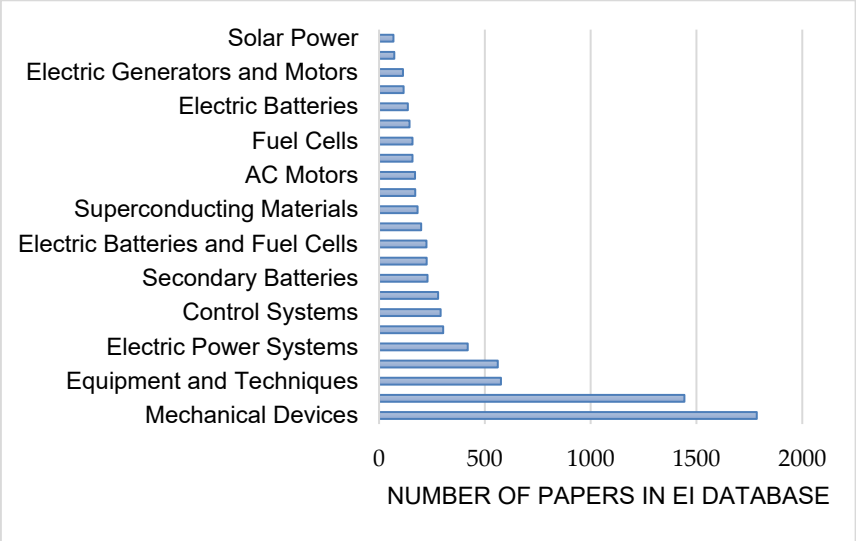

(c)

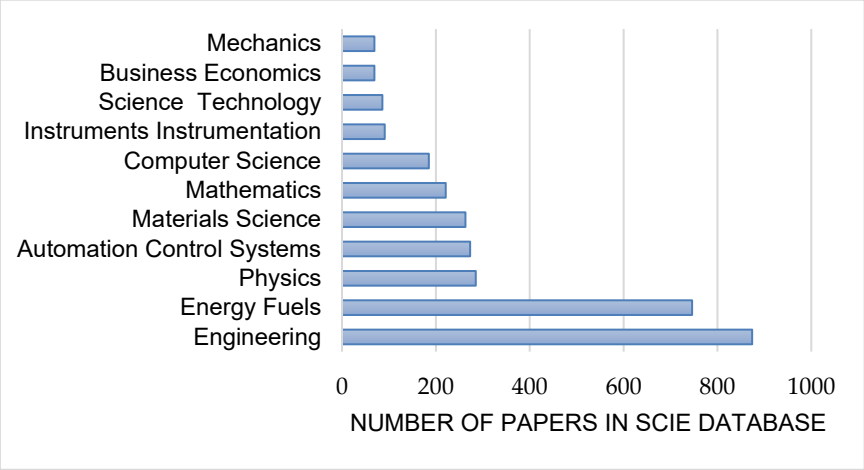

(d)

Figure 1. Literature search analysis: (a) Distribution map of published papers; (b) Distribution map of published papers' country (area) in Web of science; and (c) and (d) Number of papers in EI/SCI database.

As shown in Figure 1, in CNKI, Engineering Village, and Web of Science databases, there were 23, 257, and 0 papers, respectively, on flywheel energy storage before 2000. After 2000, the number of journal articles on "Flywheel energy storage" increased rapidly. It can be seen that flywheel energy storage technology has developed rapidly in the past 20 years, especially in the electric power industry, mechanical equipment, and energy. Figure 1(b) shows the country (region) distribution of all the data in the Web of Science database. The top five countries are China, the United States, Japan, South Korea, and the United Kingdom.

Flywheel energy storage is a mechanical energy storage technology with high power, fast response, high frequency and long life, which is suitable for transportation (rail transit [5–7], ship [8,9], automobile [10–13], aviation [14,15]), power grid quality management [16–19], wind power generation [20–22], and potential energy recovery of drilling rig [23]. Reference [10] indicates that it

has been observed that the flywheel has great potential in reducing power (load) capacity. The charging time of the vehicle and the flywheel has a significant impact on the reduction of power capacity. Reference [16] verifies the feasibility and control stability of installing a high-speed flywheel in a DC link to achieve a fast response for recovery and clipping. The principle of flywheel energy storage is to obtain energy by accelerating the rotor. According to the principle of energy conservation, the rotor continuously slows down to release energy to the outside, which is especially suitable for power-type energy storage fields [24], such as power quality control, UPS, frequency modulation, etc., and its performance is better than battery energy storage.

Flywheel materials have high specific strength requirements because they are high-speed rotating element. Due to the advantages of large total energy storage, high power and easy manufacturing, metal flywheel rotors are widely used in the industrial field. The cast iron flywheel rotor developed by Active Power Company in the United States is shown in Figure 2 [25]. Cast iron has a wide range of sources and mature manufacturing technology, which can ensure the balance and structural integrity of the rotor assembly. It is well known that the energy storage density of flywheel rotor is proportional to its strength. With the improvement of the specific strength requirements for rotor materials in various fields, high-strength wrought iron, steel and aluminum alloy materials have been developed and applied [26–28]. The UPS Power Bridge system (low-speed steel flywheel) was introduced by Piller of Germany in 1996， its capacity for a single UPS is 4.6 kW·h, and the peak Power can reach 1.6 MW [29,30]. In 1984, Japan built the world's largest flywheel energy storage system-the 215 MW/1.1MW·h flywheel system (low-speed steel), which was successfully applied in the JT-60 nuclear fusion reactor project [31].

For metal flywheel energy storage system, the research content mainly focuses on shape optimization [32], while composite flywheel has always been a hot topic due to the correlation between material designability, material properties and process [33,34]. In 2002, Arnold et al. [35] provided an elastic stress analysis of single/multi-disc, annular/solid disc and anisotropic/isotropic disc flywheels under boundary pressure, interference and centrifugal load, and discussed the influence of material properties, thickness, radius ratio and other parameters on stress. Perez-aparicio et al. [36] proposed a differential equation for composite flywheel rotors in order to accurately estimate the internal stress of the rotor. Tzeng J et al. [37] developed an analysis program for predicting elastic and viscoelastic behaviors in the flywheel design process to assess the long-term durability characteristics of composite flywheels and the potential failure mechanism of these systems. Tsinghua University [38,39] developed composite flywheel energy storage system in 1997, 2006, and 2015, respectively, using glass fiber and carbon fiber hybrid gradient materials.

Figure 2. The cast iron flywheel of active power.

In the 1970s, the US Department of Energy proposed the Super Flywheel energy storage program for vehicle power to vigorously study the flywheel technology with high energy density [40]. The flywheel can assist the hybrid drivetrain to meet the large peak power demand of heavy vehicles effectively. The Kinerstor Project aims to build and test fully at rig level a kinetic energy store, and its innovation lies in the design of the magnetic gears [40]. Tribology Systems, Inc. has developed a patented bearing and a fully mechanized rotor dynamics control system [40]. The University of Texas at Austin designed, manufactured and tested a composite flywheel battery [40]. Williams Hybrid Power Ltd (WHP) develops and manufactures electro-mechanical composite flywheel systems. WHP's flywheel solution employs its unique and patented "Magnetically Loaded Composite Material" (MLC) technology [40]. Although these companies have made innovative contributions in terms of flywheel materials, bearings or magnetic flywheels, this paper designs a high specific energy flywheel device from the perspective of multi-level flywheels. Under typical urban driving conditions, the flywheel can provide quite high auxiliary power to the vehicle for a short time during acceleration and hill climbing. During regenerative braking, the flywheel absorbs regenerative braking power much more efficiently than the battery alone. When the power required to drive the vehicle is lower than that provided by the vehicle's main power source, the excess energy can be absorbed by the flywheel. The power load balancing ability of the flywheel is vitally important for energy/power conversion and management. For automotive application of the flywheel, it is particularly important to explore how to increase the moment of inertia of the flywheel as much as possible while ensuring that the overall mass increase is minimal. In this paper, a multistage flywheel energy storage device was designed to improve the energy density and power density of the flywheel, and the parameters of both first stage and the second stage flywheel were selected reasonably, which provided a theoretical basis and design method for designing and analyzing of the multistage flywheel energy storage device.

2. Flywheel energy storage characteristics

As a rotating mechanical element, the physics of the flywheel is simple. The flywheel gains momentum after applying torque and begins to rotate, and the rotor continues to rotate after the initial torque is removed. After overcoming the friction force and air resistance of the bearing, the remaining kinetic energy drives the parts connected to it. In this process, the kinetic energy (E_{st}) stored by the flywheel and the output kinetic energy (E_{de}) are shown in Eq (1).

$$\begin{cases} E_{st} = \dfrac{1}{2} I \omega_{max}^2 \\ E_{de} = \dfrac{1}{2} I (\omega_{max}^2 - \omega_{min}^2) \end{cases} \tag{1}$$

where, I is the inertia of the flywheel, and ω_{max} and ω_{min} are the maximum and minimum angular velocity of the flywheel, respectively.

The weight of the flywheel is limited by the lightweight nature of the automobiles and the layout of the transmission system, and its size is not too large. According to Eq (1), the flywheel speed needs to be increased to maximize the stored energy of the flywheel system, that is, most of the energy（E_{st}）is stored at high speed. The output energy of flywheel energy storage system decreases rapidly with a decrease in speed, and the lower limit of running speed will affect cycle fatigue life of rotor. The literature [41,42] shows that the stored energy is useful only when the flywheel operating angular velocity ratio（$\omega_{min}/\omega_{max}$）reaches 1/3. Figure 3 shows the relationship between E_{de}/E_{st} and $\omega_{min}/\omega_{max}$.

For flywheel applications in automobiles, this speed ratio can reach 1/2. As seen in Figure 3, when the operating angular velocity reaches 1/3 and 1/2 of ω_{max}, the output storage energy is 89% and 75% of E_{st}, respectively.

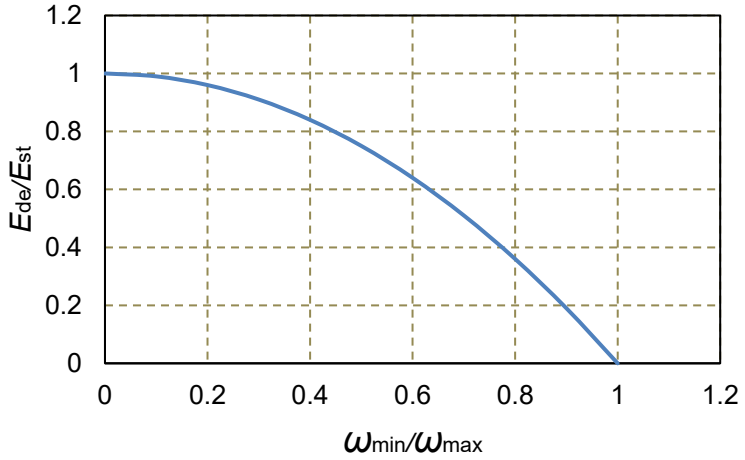

Figure 3. Relation between E_{de}/E_{st} and $\omega_{min}/\omega_{max}$.

The high-strength flywheel rotor is made of fiber-reinforced composite materials, and the flywheel is able to rotate at very high angular velocities, which enables the flywheel to meet the kinetic energy storage requirements with a small amount of inertia (or mass). To simplify the analysis, it can be considered that all the rim mass of an idealized flywheel is concentrated on a thin ring with radius r, as shown in Figure 4. The inertia of the thin ring is then mr^2 [43]. For thin rims, it is realistic to consider this problem with an idealized rotor with all mass concentrated at radius r. However, for different thicknesses of the rim, the stress field of the rotor is much more complex. In reference [44], the radial and hoop stresses (σ_r, σ_t) of the flange with different thickness at r from the central axis are given.

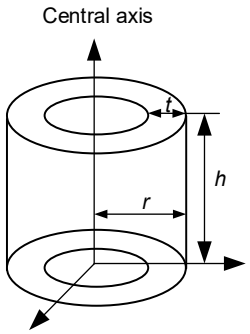

Figure 4. Idealized flywheel (thickness is t, width is h).

$$I=\int_{r_i}^{r_o}\rho\cdot 2\pi h r^3 \mathrm{d}r \tag{2}$$

$$\begin{cases}\sigma_r=\dfrac{3+\mu}{8}(r_i^2+r_o^2-r^2-\dfrac{r_i^2r_o^2}{r^2})\rho\omega^2\\ \sigma_t=\dfrac{3+\mu}{8}(r_i^2+r_o^2-\dfrac{1+3\mu}{3+\mu}r^2+\dfrac{r_i^2r_o^2}{r^2})\rho\omega^2\end{cases} \tag{3}$$

where, m is the disc total mass, ρ is the ring density, μ is Poisson's ratio, and r_i and r_o are the inner and outer radii of the disc, respectively.

According to Eq (3), the flywheel radial stress reaches its maximum when $r=\sqrt{r_i r_o}$ and is zero at the inner and outer radii, while the maximum hoop stress is obtained at the inner radius. For the rotor with variable thickness, a detailed analysis is performed using finite element software. Figure 5 shows the disc shape factor (K) of different cross section geometry, for example the K of the constant-stress disc is twice the thin ring. However, the cross-sectional shape of the rotor is complex, and it is not conducive to manufacturing process to mass production, so the section of the rim shape should comprehensively consider specific energy, processing and manufacturing technology and other factors. The calculation formula for the moment of inertia of the hollow cylinder is shown in Eq (2), and the specific energy of the thick rim under different radius ratios can be obtained by entering Eq (1). The relationship between flywheel specific energy and radius ratio at different rim linear velocities are shown in Figure 6. When the radius ratio decreases from 1.0 to 0.6, the flywheel specific energy changes rapidly. For example, when $r_i/r_o = 0.6$, the flywheel specific energy is about 0.68 times that of the thin ring ($r_i/r_o = 1.0$). Table 1 shows the maximum specific energy of the thin ring flywheel with different materials.

$$\frac{E_{st}}{m}=\frac{v^2}{4}\left[1+\left(\frac{r_i}{r_o}\right)^2\right] \tag{4}$$

where, v is the linear velocity of the outer diameter of the rim.

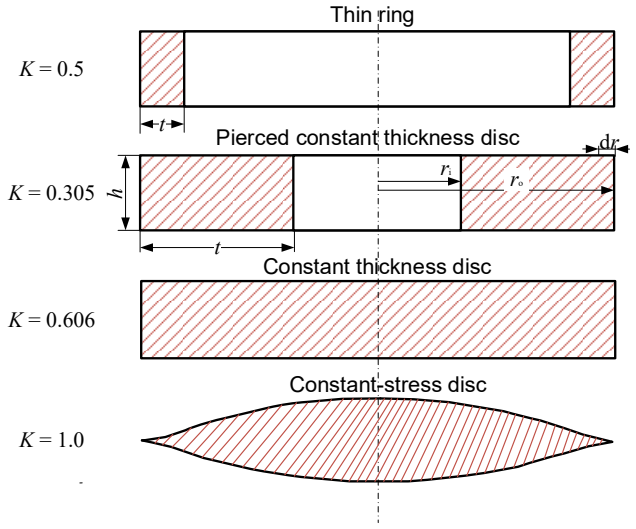

Figure 5. Several flywheel cross-sectional shape factors (thickness = t) [43,45,46].

Table 1. Properties of isotropy materials for flywheel (K = 0.5) [40,47,48].

Flywheel material	Density (kg/m^3)	Tensile stren-gth (Mpa)	Maximum specific energy (W·h/kg)	Max peripheral velocity(m/s)
Cast iron	7800	150	2.5	134
Iron 360	7800	360	2.1	123
Carbon steel	7850	340	6.0	208
Aluminum 7075	2800	469	23.3	409
Titanium Ti-6A1-4V	4430	965	30.3	467
Steel 4340	7700	1500	27.1	441
Maraging steel 18Ni-400	8000	2337	28.0	449
E-glass/epoxy	2150	1679	108.0	884
AS4 carbon/epoxy	1610	2111	182.0	1145
IM9 carbon/epoxy	1620	2993	257	1360

Notes: Weights of all flywheels were set to 1 kg, and strengths for metal rims was measured at a thickness of 1 inch.

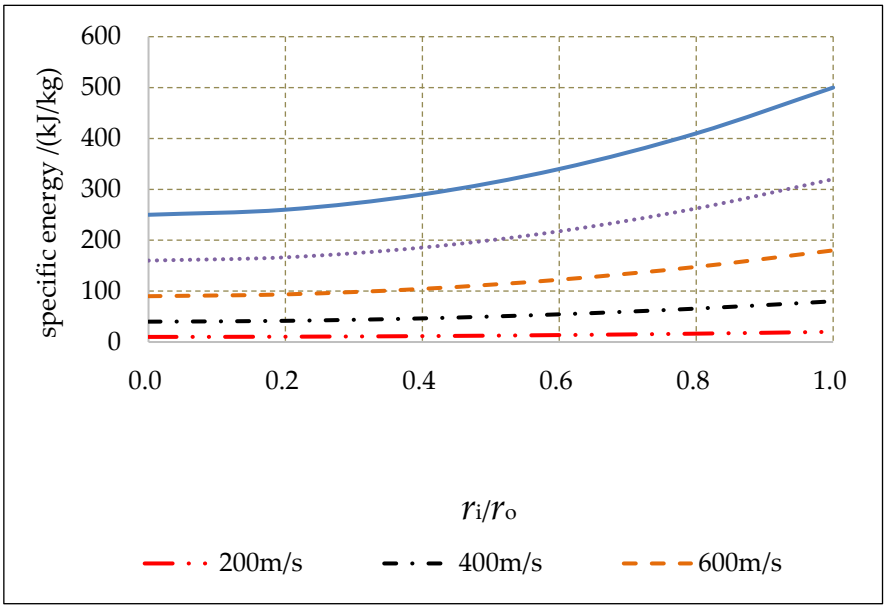

Figure 6. The relation between specific energy vs radius ratio.

3. Multistage flywheel energy storage device design

In the mechanical rotating disc model, under the same diameter and rotational speed, the maximum stress of a hollow disc with a certain inner diameter ratio will be about twice as high as that of a solid disc [21]. Therefore, under the same strength conditions, the solid disc can have a higher speed, and the required inertia will be much smaller than that of hollow disc when the energy storage is the same, thus the solid disc structure is adopted in this paper. Eq (3) shows that the maximum angular velocity of the disc rotor is limited by material strength, and the maximum angular velocity of the solid metal disc rotor (ω_{max}) satisfies Eq (5).

$$\begin{cases} \omega_{\max} r_o = \sqrt{\dfrac{8\sigma_{\max}}{\rho(3+\mu)}} \\ \sigma_{\max} \le [\sigma] \end{cases} \tag{5}$$

where, $\sigma_{\max} = \{\sigma_r, \sigma_t\}$, $[\sigma]$ is allowable tensile strength.

3.1. Two scenarios

According to the basic principle of flywheel energy storage, the amount of stored energy is proportional to the flywheel's moment of inertia and the square of its speed. Moreover, the inertia is proportional to the flywheel's mass and the square of the radius. The mass of the flywheel is limited by the lightweight nature of the automobiles and the layout of the powertrain system, so the size cannot be too large. How to improve the inertia of the flywheel as much as possible without increasing the overall mass, is particularly important. Affected by the strength of ordinary steel materials, the linear velocity of flywheel edge is limited within the range of 200 m/s, so the increase of flywheel radius is limited. Unless the flywheel is made of high-strength carbon fiber material, the radius of the flywheel can be increased. Therefore, in order to improve the performance of flywheel energy storage device, the general technical approach is to increase the speed of the flywheel, and use magnetic levitation and vacuum technology to minimize the friction loss and wind loss of the flywheel rotor. The multistage flywheel energy storage device designed in this paper adopts a two-stage flywheel on the basis of the above flywheel energy storage device, forming a flywheel energy storage device with light weight and large equivalent moment of inertia, which improves the specific energy and power density of the flywheel. Figure 7 is the schematic diagram of two kinds of multistage flywheel energy storage devices.

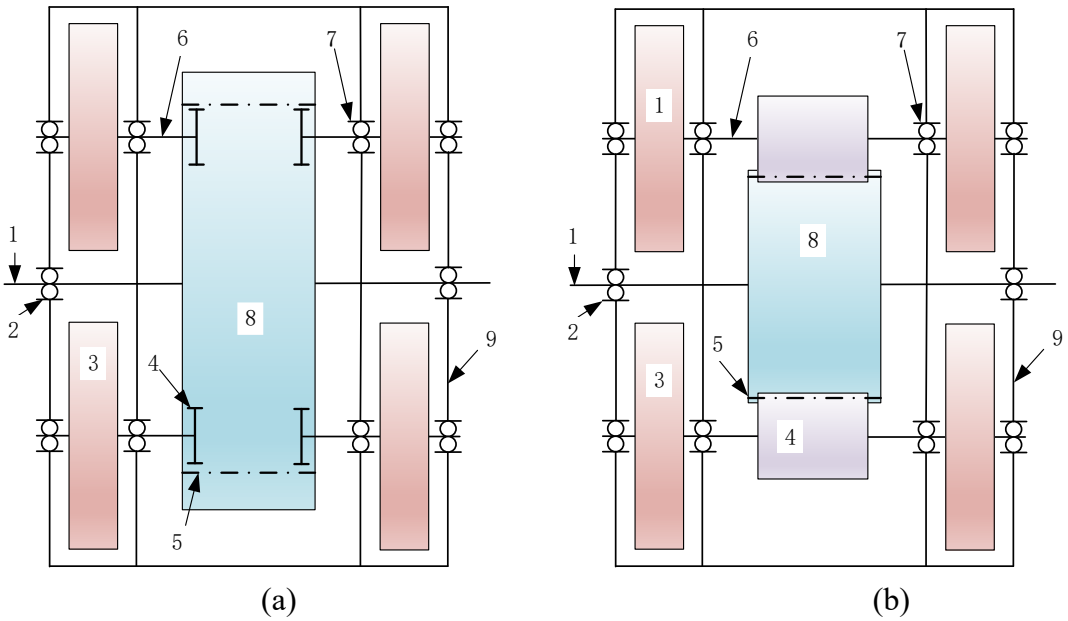

Figure 7. Schematic diagram of two kinds of multistage flywheel energy storage devices: (a) Internal gear drive; and (b) external gear drive.

As shown in Figure 7(a), the first-stage flywheel shaft (1) is installed on the bearing (2) at both ends of the box (9). The first-stage flywheel (8) is fixed on the shaft (1), and flywheel (8) is processed

with a concentric gear (5) with radius r_1 (inner gear ring). The second-stage gear (4) with the radius r_3 is internally engaged with the first-stage gear (5). The gear (4) is fixed on the second-stage flywheel shaft (6) and finally on the supporting bearing (7). The second-stage flywheel (3) with radius r_2 is fixed on the shaft (6), that is, flywheel (3) and the gear (4) are coaxially fixed on the shaft (6). Figure 7(b) shows the schematic diagram of a multistage flywheel energy storage device driven by external meshing gear. The difference from Figure 7(a) is that the first-stage gear (5) is externally meshing with the second-stage gear (4), and the others are the same as Figure 7(a).

In order to maximize the specific energy of the two-stage flywheel energy storage device, the parameters of the two-stage flywheel and gear ratio should be selected reasonably. According to the principle that the kinetic energy of the system remains unchanged before and after conversion, the total stored kinetic energy (E_{st}) and equivalent rotational inertia (I_0) of the flywheel energy storage device meet the following equation:

$$\begin{cases} E_{st} = \dfrac{1}{2} I_1 \omega_1^2 + \dfrac{1}{2} I_2 \omega_2^2 \\ E_{st} = \dfrac{1}{2} I_0 \omega_1^2 \end{cases} \Rightarrow I_0 = I_1 + I_2 \left(\frac{\omega_2}{\omega_1} \right)^2 \tag{6}$$

where I_1 and I_2 are the inertia of flywheel 8 and flywheel 3, m_1 and m_2 are the mass of flywheel 8 and flywheel 3, and ω_1 and ω_2 are the angular velocity of gear 5 and gear 4. Assuming that $\varepsilon = m_1/m_2$, $\delta = r_1/r_2$, $i = \omega_2/\omega_1$, then the I_0 and m_t are obtained as follows:

$$\begin{cases} I_0 = \dfrac{1}{2} m_1 r_1^2 \left[1 + \dfrac{i^2}{\varepsilon \delta^2} \right] = \left[1 + \dfrac{i^2}{\varepsilon \delta^2} \right] I_1 \\ m_t = m_1 + m_2 = (1 + \dfrac{1}{\varepsilon}) m_1 \end{cases} \tag{7}$$

When $i^2 \geq \varepsilon \sigma^2$, the overall mass of the flywheel energy storage device only increases by m_1/ε, but the equivalent inertia increases $\frac{i^2}{\varepsilon \delta^2} I_1$. If there are p groups of second-stage flywheels in the device, the I_0 and m_t are obtained as follows:

$$\begin{cases} I_0 = \dfrac{1}{2} m_1 r_1^2 \left[1 + \dfrac{p i^2}{\varepsilon \delta^2} \right] = \left[1 + \dfrac{p i^2}{\varepsilon \delta^2} \right] I_1 \\ m_t = m_1 + m_2 = (1 + \dfrac{p}{\varepsilon}) m_1 \end{cases} \tag{8}$$

To illustrate the advantages of flywheel energy storage device proposed in this paper quantitatively, with $i = 3$, $\varepsilon = 4$ and $\delta = 2$, and four groups of secondary flywheels are installed in the flywheel energy storage device. Therefore, the result that $I_0 = 3.25 I_1$ and $m_t = 2 m_1$ has been obtained. In this case, the specific energy of the flywheel energy storage device is as follows:

$$\begin{cases} \dfrac{E_{\mathrm{st}}^{'}}{m_{\mathrm{t}}} = \dfrac{\dfrac{1}{2} I_0 \omega_1^2}{m_{\mathrm{t}}} \\ \dfrac{E_{\mathrm{st}}}{m_1} = \dfrac{\dfrac{1}{2} I_1 \omega_1^2}{m_1} \end{cases} \Rightarrow \frac{E_{\mathrm{st}}^{'}}{m_{\mathrm{t}}} = \frac{\varepsilon\delta^2 + pi^2}{\varepsilon\delta^2 + p\delta^2} \frac{E_{\mathrm{st}}}{m_1} = 1.625 \frac{E_{\mathrm{st}}}{m_1} \tag{9}$$

According to Eq (9), the specific energy of the flywheel energy storage device designed in this paper is 1.625 times that of the original. Of course, this is not the only example.

3.2. A typical case

In order to further verify the principle in Section 3.1, a multistage flywheel energy storage device based on Figure 7(b) was made from steel 4340. According to the literature [49,50], assume that the highest speed of the first-stage flywheel in this case is 25,000 rpm, and the radius of the first-stage flywheel should be less than 263 mm calculated through Eq (5). Considering that the flywheel radius was limited by box space, the radius of the first-stage flywheel was 82.5 mm, and the its width was 24 mm. Furthermore, according to Eq (5), the radius of the second-stage flywheel should be less than 87 mm. Here, the radius was 75 mm, and the width was 30 mm. In this section, a 3D model of the flywheels was established using Siemens NX 12.0, as shown in Figure 8. The mass of the parts was measured using an analysis module, and the detailed parameters of the flywheel were obtained as shown in Table 2. Finally, according to the above parameters, a prototype of the flywheel energy storage device was designed, as shown in Figure 9.

Table 2. Flywheel energy storage device parameters.

Parts	Parameters	Value
First-stage flywheel (ring gear)	Radius/r_1(mm)	82.5
	Width/h(mm)	24
	Gear teeth	66
	Gear module	2.5
	Mass/m_1(kg)	3.77
	Numbers	2
	Inner hole(mm)	Ø40
Second-stage gear	Radius/r_3(mm)	27.5
	Width/h(mm)	24
	Gear teeth	22
	Gear module	2.5
	Mass/m_3(kg)	0.30
	Numbers	8
	Inner hole(mm)	Ø30
Second-stage flywheel	Radius/r_2(mm)	75
	Width/h(mm)	30
	Mass/m_2(kg)	3.92
	Numbers	8
	Inner hole(mm)	Ø35

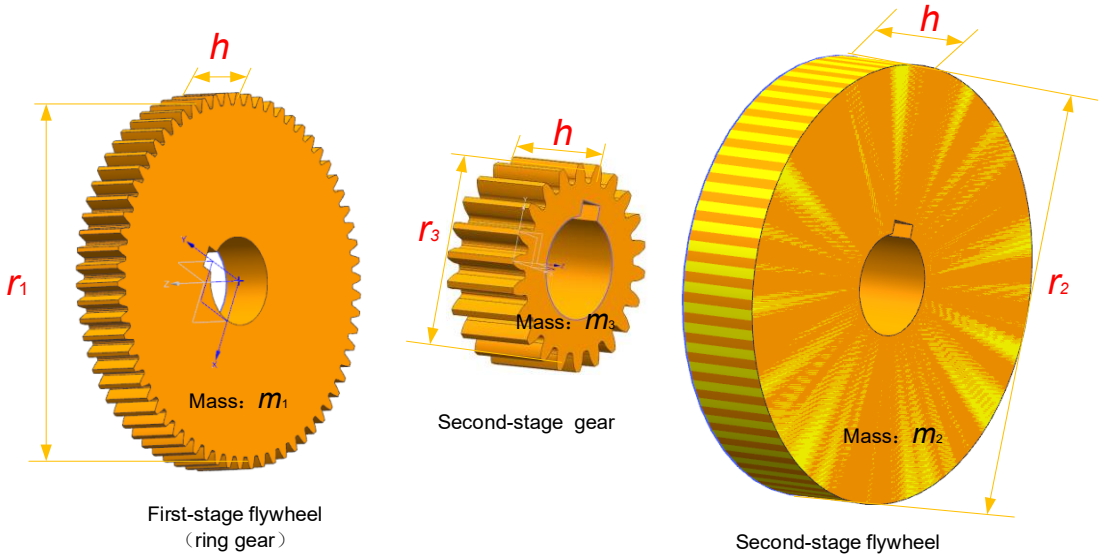

(a)

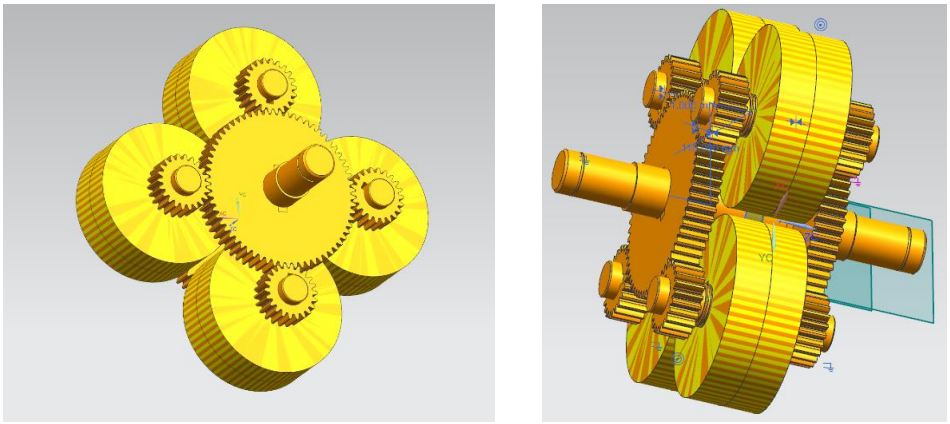

(b)

Figure 8. 3D Model of the flywheel energy storage device: (a) Flywheel model; an (b) flywheel assembly drawing model.

Figure 9. Prototype of a multistage flywheel energy storage device.

4. Discussion

In this section, we discuss some contents in the research work. It can help readers better understand the significance, value, and prospects of this research.

According to the design parameters, $i = 3$, $\varepsilon = 0.96$, and $\delta = 1.1$ are obtained, and 4 groups of secondary flywheels are designed in this paper. It can be calculated from Eq (8) that $I_0 = 32I_1$ and $m_t = 5.2m_1$. Finally, the specific energy of the multistage energy storage flywheel device can be obtained by substituting it into Eq (9) as follows:

$$\frac{E'_{st}}{m_t} = \frac{\varepsilon\delta^2 + pi^2}{\varepsilon\delta^2 + p\delta^2}\frac{E_{st}}{m_1} = 6.19\frac{E_{st}}{m_1} \tag{10}$$

Here, the results ignore the influence of the second stage gear mass in the specific energy of the flywheel device. If the mass of the second stage gear is taken into account, the specific energy of the flywheel device is 5.80 times of the original one. Moreover, under the premise of a certain ε and δ, the larger i is, the larger the specific energy is.

We focus on using a two-stage flywheel to improve the specific energy of flywheel device. In the proposed device, the characteristics of the all-metal flywheel are discussed. The flywheel rotor made of fiber-reinforced composite with high strength can rotate at very high angular velocities, which enables it to meet the demand for kinetic energy storage with less inertia (or mass). It is assumed that the design parameters of flywheel energy storage device are as shown in Table 2, and the components are made of all-composite materials, such as E-glass/epoxy and AS4 carbon/epoxy. At this time, the mass of flywheel energy storage device (including the first-stage flywheel, the second-stage gear and the second-stage flywheel) is shown in Table 3.

The mass of flywheel energy storage device made of E-glass/epoxy or AS4 carbon/epoxy is 72.54% and 81.28% lower than that of Steel 4340, respectively, which is more suitable for super flywheel energy storage for vehicle power. Therefore, this design idea provides another exploration direction for improving the performance of flywheel energy storage device.

Table 3. Flywheel energy storage device mass.

Flywheel material	First-stage flywheel (ring gear)/kg	Second-stage gear /kg	Second-stage flywheel /kg	Total mass/kg
Steel 4340	3.77	0.30	3.92	41.3
E-glass/epoxy	1.03	0.08	1.08	11.34
AS4 carbon/epoxy	0.77	0.06	0.81	7.73

5. Conclusions

At present, most researchers focus on shape optimization for metal flywheel energy storage systems. In this paper, a multistage flywheel rotor was designed to improve the specific energy of the system. For the energy storage device with certain mass, the multistage flywheel energy storage device can store more energy by choosing the parameters of the flywheel rotor reasonably. To prove this theory, the system model was established with NX12.0, and the specific energy of the system with the analysis module was obtained. Finally, the prototype of multistage flywheel energy storage device was

processed. This design idea and optimization process provided a new method for improving the flywheel specific energy.

Use of AI tools declaration

The authors declare they have not used Artificial Intelligence (AI) tools in the creation of this article.

Acknowledgments

This research was funded by the Beijing Polytechnic University Key Program (Grant No. 2024X022-KXZ), Major Project of the Natural Science Foundation of Beijing Polytechnic University (2024X007-KXD).

Conflict of interest

The authors declare no conflicts of interest.

Author contributions

Methodology, Hong Li and Jiangwei Chu; software, Xiaojiao Wang and Yueyi Li; validation, Hong Li, Junjie Chen, Wanqi Wang; writing—original draft preparation, Hong Li; writing—review and editing, Hong Li and Jjiangwei Chu. All authors have read and agreed to the published version of the manuscript.

References

1. Energy Storage Committee of China Energy Research Society. White paper of energy storage industry research 2022. *China Energy Storage Alliance*, 2022. Available from: http://www.cnesa.org/information/detail/?column_id=1&id=4567.
2. Rufer A (2017) The dream of efficient energy storage-from BESS, KERS & Co. to the hybrid power plant. *In Proceedings of the 19th European Conference on Power Electronics and Applications (EPE'17 ECCE Europe)*, 11–14. https://doi.org/10.23919/EPE17ECCEEurope.2017.8099416
3. Guney MS, Tepe Y (2017) Classification and assessment of energy storage systems. *Renew Sustain Energy Rev* 75: 1187–1197. https://doi.org/10.1016/j.rser.2016.11.102
4. Hadjipaschalis I, Poullikkas A, Efthimiou V (2009) Overview of current and future energy storage technologies for electric power applications. *Renew Sustain Energy Rev* 13: 1513–1522. https://doi.org/10.1016/j.rser.2008.09.028
5. Solis O, Castro F, Bukhin L, et al. (2015) Saving money every day: La metro subway wayside energy storage substation. *2014 Joint Rail Conference*. https://doi.org/10.1115/JRC2015-5691
6. Rupp A, Baier H, Mertiny P, et al. (2016) Analysis of a flywheel energy storage system for light rail transit. *Energy* 107: 625–638. https://doi.org/10.1016/j.energy.2016.04.051
7. Zhang W, Wu G, Rao Z, et al. (2020) Predictive power control of novel N *3-phase PM energy storage motor for urban rail transit. *Energies* 13: 1578. https://doi.org/10.3390/en13071578

8. Xie C, Zhang C, Chang J (2011) Research on simulation of ship electric propulsion system with flywheel energy storage system. *Microsyst Technol* 17: 1161–1167. https://doi.org/10.1007/s00542-011-1268-0
9. Hou J, Song Z, Hofmann H, et al. (2021) Control strategy for battery/flywheel hybrid energy storage in electric shipboard microgrids. *IEEE Trans Ind Inf* 17: 1088–1099. https://doi.org/10.1109/TII.2020.2973409
10. Erdemir D, Dincer I (2020) Assessment of renewable energy-driven and flywheel integrated fast-charging station for electric buses: A case study. *J Energy Storage* 8: 101576. https://doi.org/10.1016/j.est.2020.101576
11. Kurtulmu ZN, Karakaya A (2024) efficiency analysis of regenerative brake system using flywheel energy storage technology in electric vehicles. *Tehnicki Vjesnik-Technical Gazette* 31: 442–448. https://doi.org/10.17559/TV-20230611000719
12. Mehraban A, Ghanbari T, Farjah E (2024) Dual-inertia flywheel energy storage system for electric vehicles. *IET Electric Power Appl* 18: 1370–1381. https://doi.org/10.1049/elp2.12485
13. Thormann B, Puchbauer P, Kienberger T (2021) Analyzing the suitability of flywheel energy storage systems for supplying high-power charging e-mobility use cases. *J Energy Storage*, 39. https://doi.org/10.1016/j.est.2021.102615
14. Lu J, Zheng H, Haider MH (2023) Fracture failure analysis of flywheel hub served in heavy-fuel aviation piston engine. *Eng Failure Anal*, 107363. https://doi.org/10.1016/j.engfailanal.2023.107363
15. Zhu H, Qin J, Zhu Q, et al. (2024) The Angular momentum unloading of the asymmetric GEO satellite by using electric propulsion with a mechanical arm. *Aerospace* 11: 290. https://doi.org/10.3390/aerospace11040290
16. Lu YJ, Laribi R, Sauer A (2021) Modeling and control of an energy storage system for peak shaving in industrial pulsed power applications. *2021 Power System and Green Energy Conference* 8: 390–394. https://doi.org/10.1109/PSGEC51302.2021.9542104
17. Elbouchikhi E, Amirat Y, Feld G, et al. (2020) A lab-scale flywheel energy storage system: control strategy and domestic applications. *Energies*, 13. https://doi.org/10.3390/en13030653
18. Eltantawy AB, Salama MMA, El-Fouly THM, et al. (2015) Enhancing storage capabilities for active distribution systems using flywheel technology. *Electr Compon Syst* 43: 1133–1140. https://doi.org/10.1080/15325008.2014.990069
19. Tziovani L, Hadjidemetriou L, Charalampous C, et al. (2021) Energy management and control of a flywheel storage system for peak shaving applications. *IEEE Trans Smart Grid* 12: 4195–4207. https://doi.org/10.1109/TSG.2021.3084814
20. Lai J, Song Y, Du X (2018) Hierarchical coordinated control of flywheel energy storage matrix systems for wind farms. *IEEE/ASME Trans Mechatron* 23: 48–56. https://doi.org/10.1109/TMECH.2017.2654067
21. Hutchinson A, Gladwin DT (2020) Optimisation of a wind power site through utilisation of flywheel energy storage technology. *Energy Rep* 6: 259–265. https://doi.org/10.1016/j.egyr.2020.03.032
22. Diaz-Gonzalez F, Sumper A, Gomis-Bellmunt O, et al. (2013) Energy management of flywheel-based energy storage device for wind power smoothing. *Appl Energy* 110: 207–219. https://doi.org/10.1016/j.apenergy.2013.04.029
23. Dai X, Wei K, Zhang X (2019) Analysis of the peak load leveling mode of a hybrid power system with flywheel energy storage in oil drilling rig. *Energies* 12: 606. https://doi.org/10.3390/en12040606

24. Doucette RT, Mcculloch MD (2011) A comparison of high-speed flywheels, batteries, and ultracapacitors on the bases of cost and fuel economy as the energy storage system in a fuel cell based hybrid electric vehicle. *J Power Sources* 196: 1163–1170. https://doi.org/10.1016/j.jpowsour.2010.08.100
25. Wu X, Chen Y, Liu Y (2021) Structure optimization of metal rotor of grid-connected flywheel energy storage system. *Acta Energ Sol Sin* 42: 317–321. https://doi.org/10.19912/j.0254-0096.tynxb.2018-0907
26. Post RF (1996) A look at an old idea: The electromechanical battery. *Sci Technol Rev* 4: 13. Available from: https://www.researchgate.net/publication/236439955.
27. Li X, Anvari B, Palazzolo A, et al. (2017) A utility scale flywheel energy storage system with a shaft-less, hub-less, high strength steel rotor. *IEEE Trans Ind Electron*. https://doi.org/10.1109/TIE.2017.2772205
28. Tang J, Zhang Y, Ge SS, et al. (2013) Hollow interference fitted multi-ring composite rotor of the superconducting attitude control and energy storage flywheel. *J Reinf Plast Compos* 32: 881–897. https://doi.org/10.1177/0731684413480009
29. Werfel FN, Floegel-Delor U, Rothfeld R, et al. (2011) Superconductor bearings, flywheels and transportation. *Supercond Sci Technol* 25: 14007–14022. https://doi.org/10.1088/0953-2048/25/1/014007
30. Werfel FN, Floegel-Delor U, Riedel T, et al. （2010） HTS magnetic bearings in prototype application. *IEEE Trans Appl Supercond* 20: 874–879. https://doi.org/10.1109/TASC.2010.2040261
31. Tang C, Zhang X, Meng X (2018) Research on flywheel energy storage technology abroad. *Sino-Global Energy* 23: 82–86. Available from: https://xueshu.baidu.com/usercenter/paper/show?paperid=147q0mr0050c0pv0my5p0r201d698270&site=xueshu_se&hitarticle=1.
32. Daniel C, Fabio da SB, Joao MLM, et al. (2024) Optimization of flywheel rotor energy and stability using finite element modelling. *Energies* 17: 3042. https://doi.org/10.3390/en17123042
33. Yangoz C, Erhan K (2025) High-speed kinetic energy storage system development and ANSYS analysis of hybrid multi-layered rotor structure. *Appl Sci* 15: 5759. https://doi.org/10.3390/app15105759
34. Xu K, Guo Y, Lei G, et al. (2023) A review of flywheel energy storage system technologies. *Energies* 2023: 6462. https://doi.org/10.3390/en16186462
35. Arnold SM, Saleeb AF, Al-Zoubi NR (2002) Deformation and life analysis of composite flywheel disk systems. *Compos Part B: Eng* 33: 433–459. https://doi.org/10.1016/S1359-8368(02)00032-X
36. Perez-Aparicio JL, Ripoll L (2011) Exact, integrated and complete solutions for composite flywheels. *Compos Struct* 93: 1404–1415. https://doi.org/10.1016/j.compstruct.2010.11.011
37. Tzeng J, Emerson R, Moy P (2006) Composite flywheels for energy storage. *Compos Sci Technol* 66: 2520–2527. https://doi.org/10.1016/j.compscitech.2006.01.025
38. Dai X, Zhang X, Jiang X, et al. (2012) Flywheel energy storage technology in Tsinghua University. *Energy Storage Sci Technol* 1: 64–68. Available from: https://xueshu.baidu.com/usercenter/paper/show?paperid=cb3d2deecd124d4a1ce9277ba5db15d2&site=xueshu_se&hitarticle=1.
39. Dai X, Wei K, Zhang X, et al. (2018) A review on flywheel energy storage technology in fifty years. *Energy Storage Sci Technol* 7: 765–782. Available from: https://webofscience.clarivate.cn/wos/cscd/full-record/CSCD:6326626.

40. Hansen JGR, O'Kain Du (2012) An assessment of flywheel high power energy storage technology for hybrid vehicles. *Oak Ridge: National Laboratory*, 2012. Available from: https://info.ornl.gov/sites/publications/Files/Pub31707.pdf.
41. Ruddell A (2003) Storage technology report: WP-ST6 flywheel in investigation on storage technologies for intermittent renewable energies: Evaluation and recommended R&D strategy. *European Community 5th Framework Programme Contract* No. ENK5-CT-2000- 20336, June 17, 2003. Available from: https://api.semanticscholar.org/CorpusID:13609385.
42. Butler P, Dipietro P, Johnson L, et al. (1999) A summary of the state of the art of superconducting magnetic energy storage systems, flywheel energy storage systems, and compressed air energy storage systems. Available from: https://api.semanticscholar.org/CorpusID:117517983.
43. Amiryar ME, Pullen KR (2017) A review of flywheel energy storage system technologies and their applications. *Appl Sci* 7: 1–21. https://doi.org/10.3390/app7030286
44. Ugural AC, Fenster SK (1979) Advanced strength and applied elasticity. *Elsevier North Holland Publishing Company*, Inc., New York. Available from: https://web.njit.edu/~me/ME%20437%20PDF.pdf.
45. Thoolen F (1993) Development of an advanced high speed flywheel energy storage system. Available from: http://alexandria.tue.nl/repository/books/406829.pdf.
46. Bolund B, Bernhoff H, Leijon M (2007) Flywheel energy and power storage systems. *Renewable Sustainable Energy Rev* 11: 235–258. https://doi.org/10.1016/j.rser.2005.01.004
47. Dragoni E (2019) Mechanical design of flywheels for energy storage: A review with state-of-the-art developments. *Proc Inst Mech Eng, Part L: J Mater: Des Appl* 233: 995–1004. https://doi.org/10.1177/1464420717729415
48. Kong D, Pei Y, Xing L, et al. (2014) Metallic materials for energy storage flywheel rotors. *Energy Storage Sci Technol*, 2014. Available from: https://api.semanticscholar.org/CorpusID:137716684.
49. Changzhou Haike New Energy. *Recycling kinetic energy propulsion system—"electrical type" flywheel KERS*, Chang zhou, China, 2012. Available from: http://www.chk-net.com/en/product.asp?id=11.
50. Volvo car group. Volvo Car Group and Flybrid Conduct UK Testing of Flywheel KERS Technology. Available from: https://www.media.volvocars.com/uk/en-gb/media/pressreleases/141626/volvo-car-group-and flybrid-conduct-uk-testing-of-flywheel-kers-technology.